Erschienen in: Plant and Cell Physiology ; 55 (2014), 4. - S. 727-736
https://dx.doi.org/10.1093/pcp/pcu019

The ESCRT-III-Interacting Deubiquitinating Enzyme AMSH3 is Essential for Degradation of Ubiquitinated Membrane Proteins in *Arabidopsis thaliana*

Anthi Katsiarimpa[1,4], Alfonso Muñoz[2], Kamila Kalinowska[1], Tomohiro Uemura[3], Enrique Rojo[2] and Erika Isono[1,4,*]

[1]Department of Plant Systems Biology, Technische Universität München, D-85354,Freising, Germany
[2]Department of Plant Molecular Genetics, Centro Nacional de Biotecnología, CNB-CSIC, Madrid 280049, Spain
[3]Department of Biological Sciences, Graduate School of Science, University of Tokyo, Tokyo, 113-0033 Japan
[4]These authors contributed equally to this work.
*Corresponding author: E-mail, erika.isono@wzw.tum.de; Fax, +49 8161 712886.

Post-translational modification by ubiquitin plays a key role in the regulation of endocytic degradation in which ubiquitinated plasma membrane cargos are transported to the vacuole for degradation dependent on the ESCRT (endosomal sorting complex required for transport) machinery. Arabidopsis AMSH3 (ASSOCIATED MOLECULE WITH THE SH3 DOMAIN OF STAM 3) is a deubiquitinating enzyme that interacts with at least two subunits of the ESCRT-III machinery, VPS2.1 and VPS24.1. *amsh3* null mutation causes seedling lethality, and *amsh3* null mutants show defects in multiple intracellular trafficking pathways. In this study, we further analyzed the *amsh3* mutant phenotype and showed that *amsh3* accumulates membrane-associated ubiquitinated proteins, supporting the indication that AMSH3 functions in ubiquitin-mediated endocytic degradation. In accordance with this, an enzymatic inactive variant of AMSH3 inhibits the AvrPtoB-dependent endocytic degradation of CERK1 (CHITIN ELICITOR RECEPTOR KINASE 1). Furthermore, we showed that the interaction of AMSH3 with ESCRT-III is important for its function in planta. Together, our data indicate the importance of AMSH3 and the AMSH3–ESCRT-III interaction for deubiquitination and degradation of ubiquitinated membrane substrates in plants.

Keywords: AMSH • *Arabidopsis thaliana* • ESCRT • Ubiquitin.

Abbreviations: AMSH, ASSOCIATED MOLECULE WITH THE SH3 DOMAIN OF STAM; BFA, brefeldin A; CERK1, CHITIN ELICITOR RECEPTOR KINASE 1; DEX, dexamethasone; DUB, deubiquitinating enzyme; ESCRT, endosomal sorting complex required for transport; FLS, FLAGELLIN-SENSITIVE; GFP, green fluorescent protein; GST, glutathione *S*-transferase; MIM, MIT-interacting motif; MIT, microtubule interacting and transport; MVB, multivesicular body; PIN, PIN-FORMED; PI3K, phosphoinositide 3-kinase; SKD, SUPPRESSOR OF K+ TRANSPORT GROWTH DEFECT; SNF, SUCROSE NONFERMENTING; VPS, VACUOLAR PROTEIN SORTING; WM, wortmannin.

Introduction

Plasma membrane proteins are important for the coordination of extracellular stimuli and intracellular signaling pathways, and thus the regulation of their abundance and activity is critical to control downstream signaling events. Recent studies have shown that ubiquitination also regulates endocytosis and the subsequent vacuolar degradation of plasma membrane proteins in plants. Evidence has been provided for ubiquitin-dependent endocytosis for a number of plant plasma membrane-localized proteins, among others CHITIN ELICITOR RECEPTOR KINASE 1 (CERK1), REQUIRES HIGH BORON 1 (BOR1), FLAGELLIN-SENSITIVE 2 (FLS2), IRON-REGULATED TRANSPORTER 1 (IRT1) and PIN-FORMED 2 (PIN2) (Abas et al. 2006, Gohre et al. 2008, Lee et al. 2009, Barberon et al. 2011, Kasai et al. 2011). It was also shown that translational fusion of a single ubiquitin moiety to a plasma membrane ATPase was sufficient for endocytosis and targeting to the vacuole (Herberth et al. 2012, Scheuring et al. 2012).

Studies in yeast and mammals have revealed the mechanisms by which the ubiquitin-binding domains of the endocytosis machinery recognize and bind the ubiquitinated cargo and eventually sort them into the intraluminal vesicles of multivesicular bodies. This process requires an intact endosormal sorting complex required for transport (ESCRT)-0, I, II and III (reviewed in Williams and Urbe 2007). Homologs of all ESCRT components, except those of ESCRT-0, can be identified by homology search in the *Arabidopsis thaliana* genome

(Winter and Hauser 2006, Schellmann and Pimpl 2009). ESCRT-III consists of four core subunits VACUOLAR PROTEIN SORTING 20 (VPS20), SUCROSE NONFERMENTING 7 (SNF7), VPS2 and VPS24, which were shown to assemble in an ordered manner on the limiting membrane of multivesicular bodies (MVBs) in yeast (Teis et al. 2008). Recent results suggest that Arabidopsis ESCRT proteins are also pivotal for the MVB sorting pathway and essential for proper plant development. For example, a mutant of an ESCRT-I subunit *elch*/*vps23* shows defects in cytokinesis (Spitzer et al. 2006) and a mutant of one of the ESCRT-III-associated proteins *chmp1a/b* (*vps46*) has defects in embryo development and is defective in the delivery of PIN1, PIN2 and AUX1 to the vacuole (Spitzer et al. 2009). An ESCRT-III core component mutant *vps2.1* shows embryo lethality (Katsiarimpa et al. 2011), implying the essential function of ESCRT-III in plants.

Ubiquitination is a reversible post-translational modification. A cascade of E1, E2 and E3 enzymes work together to conjugate ubiquitin to the target protein, and this modification can be reversed by the activity of deubiquitinating enzymes (DUBs). Some DUBs play a role in ubiquitin precursor processing, and DUB activity also guarantees the recycling of ubiquitin molecules prior to degradation of the substrate proteins. One essential function of DUBs is therefore contributing to the maintenance of the free ubiquitin level in the cell. However, since ubiquitination regulates a broad range of cellular events, DUBs also play active roles in controlling the stability of their substrate proteins and thus in the regulation of various aspects of plant biology. Indeed, DUB function was shown to be required for different stages of plant development and physiology (Yan et al. 2000, Doelling et al. 2001, Doelling et al. 2007, Sridhar et al. 2007, Liu et al. 2008, Luo et al. 2008, Schmitz et al. 2009).

Eukaryotic DUBs can be classified into five distinct families (Komander et al. 2009), the MPR1, PAD1 N-terminal+/JAB1/MPN/MOV34 (MPN+/JAMM) domain family being one of them (Maytal-Kivity et al. 2002, Ambroggio et al. 2004, Clague and Urbe 2006, Komander et al. 2009). AMSH (ASSOCIATED MOLECULE WITH THE SH3 DOMAIN OF STAM) proteins are highly conserved DUBs of the MPN+ family whose function is implicated in intracellular trafficking both in mammals (Tanaka et al. 1999, Ishii et al. 2001, McCullough et al. 2004, McCullough et al. 2006, Ma et al. 2007, Sato et al. 2008, Hasdemir et al. 2009, Sierra et al. 2010, Huang et al. 2013) and in plants (Isono et al. 2010, Katsiarimpa et al. 2011, Katsiarimpa et al. 2013).

Arabidopsis has three AMSH homologs named AMSH1, AMSH2 and AMSH3. We have recently shown that a knockdown mutant of *amsh1* is defective in authophagic degradation whereas *amsh3* null mutation causes seedling lethality (Isono et al. 2010, Katsiarimpa et al. 2013). At the intracellular level, *amsh3* mutants show a number of defects in intracellular trafficking. In this study, we further analyzed the phenotype of *amsh3* mutants in intracellular trafficking at both the cell biological and the biochemical level. *amsh3* mutants showed an altered response upon pharmaceutical inhibition of intracellular trafficking with brefeldin A (BFA) and wortmannin (WM), accumulated membrane-bound ubiquitinated proteins, and co-expression of enzymatic inactive AMSH3 leads to the accumulation of the plasma membrane receptor kinase CERK1 upon AvrPtoB co-expression, implying AMSH3 function in ubiquitin-mediated endocytic degradation. We also show that the MIT (microtubule interacting and transport) domain of AMSH3 at its N-terminus is the interaction surface with the MIT-interacting motif (MIM) of the ESCRT-III subunit VPS2.1. Moreover, inducible expression of AMSH3(ΔMIT), in contrast to full-length AMSH3, cannot even partially rescue the *amsh3* mutant phenotype, indicating the importance of AMSH3 and the AMSH3–ESCRT-III interaction for AMSH function in plants.

Results

BFA body formation is affected in *amsh3*

amsh3 null mutants were previously shown to be defective in central vacuole biogenesis and in a number of intracellular trafficking events. For example, *amsh3* mutants show defects in transport of PIN-FORMED 2 (PIN2)–green fluorescent protein (GFP) and an artificial vacuolar cargo CT24–GFP to the vacuole (Isono et al. 2010). To examine endosomal trafficking in more detail, we analyzed the behavior of PIN2–GFP in the root epidermis cells of wild-type and *amsh3* seedlings.

Endosomal trafficking of PIN2–GFP can be pharmaceutically inhibited by treatment of seedlings with BFA, a fungal toxin and inhibitor of protein transport, or WM, an inhibitor of phosphoinositide 3-kinase (PI3K) and PI4K that inhibits endosomal trafficking. Upon BFA treatment, PIN2–GFP was shown to accumulate in BFA-induced cytosolic aggregates or so-called BFA bodies (Geldner et al. 2001, Dhonukshe et al. 2007). In wild-type root epidermis cells, large BFA bodies with a median size of 6.80 μm^2 ($n = 48$ cells) were observed after 60 min of BFA treatment (**Fig. 1A**, left panel, **Fig. 1C**). In contrast, in the *amsh3* mutants, BFA bodies were much smaller with a median size of 1.80 μm^2 ($n = 53$ cells) (**Fig. 1A**, right panel, **Fig. 1C**), suggesting that *amsh3* is defective in the formation of large PIN2–GFP-positive BFA bodies or that formation of BFA bodies is delayed in *amsh3*. Upon treatment with WM, PIN2–GFP was shown to accumulate in large ring-like structures (Jaillais et al. 2006) and, indeed, WM-induced structures appeared after 120 min of treatment and had a median area of 1.81 μm^2 ($n = 30$ cells) in wild-type cells (**Fig. 1B**, left panel, **Fig. 1D**). Under the same conditions, however, PIN2–GFP accumulated in much smaller structures with a median size of 1.18 μm^2 ($n = 52$ cells) in *amsh3* cells (**Fig. 1B**, right panel, **Fig. 1D**), suggesting that *amsh3* is also impaired in efficiently forming WM-induced structures.

To investigate further BFA body formation in *amsh3*, we examined the staining with the endocytosis tracer FM4-64 upon BFA treatment in both the wild type and *amsh3*. The seedlings were pre-incubated with FM4-64 for 10 min before treatment with BFA. The behavior of FM4-64 was imaged over

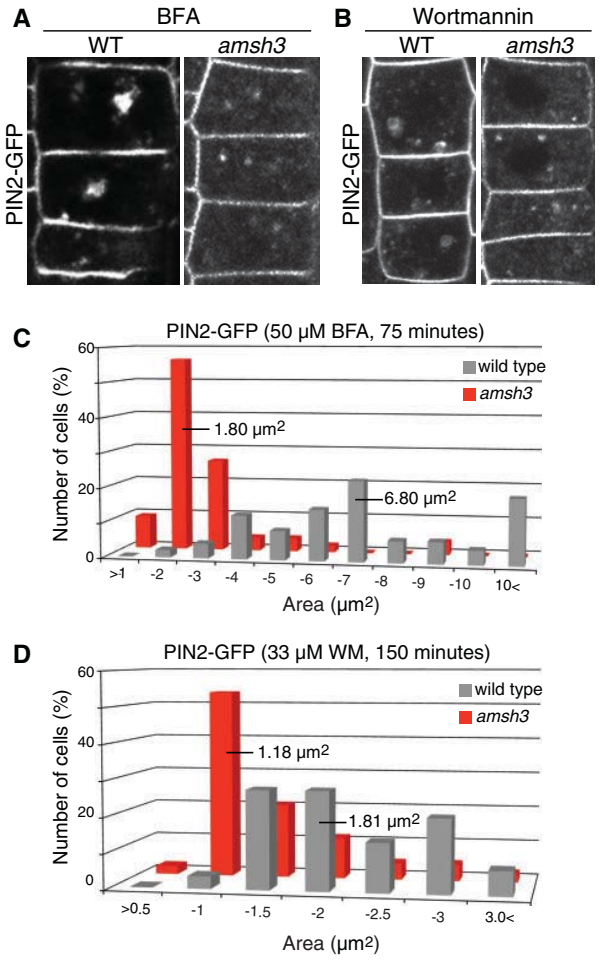

Fig. 1 PIN2–GFP accumulates in smaller BFA- and WM-induced compartments in *amsh3*. (A) PIN2–GFP localization in the wild type and *amsh3* 75 min after BFA treatment. (B) PIN2–GFP localization in the wild type and *amsh3* 150 min after WM treatment. (C) Quantification of the results in (A). The area of BFA compartments in the wild type and *amsh3* was quantified, and median values are indicated. (D) Quantification of the results in (B). The area of WM-induced compartments in the wild type and *amsh3* was quantified, and median values are indicated.

the time-course of the experiment. In wild-type seedlings, accumulation of FM4-64 became clear after 20 min (**Fig. 2**). In contrast, in *amsh3*, formation of FM4-64-stained BFA bodies was observed much later, after around 110 min. Since the uptake of FM4-64 is not delayed in *amsh3* when compared with the wild type (**Supplementary Fig. S1**), these data indicate that endosomal trafficking, especially in regard to BFA- and WM-affected factors, is somehow altered in *amsh3*.

amsh3 accumulates ubiquitinated membrane proteins

We have previously shown that *amsh3* mutants as well as a dominant-negative and enzymatic inactive AMSH3(AXA)-expressing plants accumulate ubiquitinated proteins at high

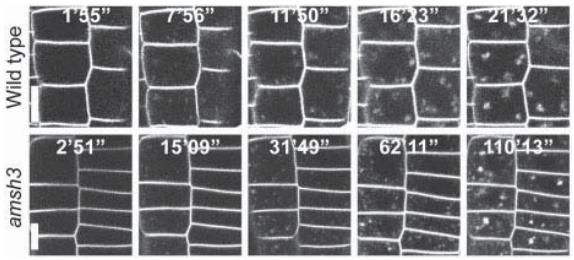

Fig. 2 BFA body formation is delayed in *amsh3*. A time-course experiment was performed using FM4-64 in the BFA-treated wild type and *amsh3*. The time after BFA treatment is indicated on top of each panel. Scale bars = 10 μm.

levels (Isono et al. 2010). If the accumulation of ubiquitinated proteins in *amsh3* were due to its defects in intracellular trafficking, pharmaceutical treatments that inhibit endocytic degradation of (ubiquitinated) membrane proteins would also cause the accumulation of ubiquitinated proteins. To test this possibility, we examined the alteration in the abundance of ubiquitinated proteins upon pharmaceutical inhibition of endocytosis. We treated wild-type seedlings with different endocytosis inhibitors, the clathrin-dependent endocytosis inhibitor tyrphostin A23 (A23), BFA, WM and the vacuole protease inhibitor E-64d. Treatment with tyrphostin A23 showed only a slight increase in ubiquitin conjugates. However, BFA and WM treatment led to the accumulation of ubiquitinated proteins at much higher levels in comparison with the mock treatment (**Fig. 3A**), indicating that general inhibition of endocytosis can indeed cause accumulation of ubiquitinated proteins, similar to inhibition of AMSH3 function. E-64d treatment leads to only moderate changes in the ubiquitin profile, suggesting that the ubiquitin chains are probably removed prior to degradation in the vacuole.

To investigate whether the accumulated ubiquitinated proteins in *amsh3* mutants are indeed membrane or membrane-associated proteins, we performed cell fractionation by ultracentrifugation with total protein extracts of wild type, *amsh3* and AMSH3(AXA)-overexpressing seedlings. Immunoblotting with an anti-ubiquitin antibody revealed that the majority of ubiquitinated proteins were enriched in the microsomal pellet fraction (P100) (**Fig. 3B, C**). The two control proteins mCherry–Rab7Gf (wave5y) (Geldner et al. 2009) and UGPase were almost exclusively found in the P100 and S100 fraction, respectively. These results indicate that ubiquitinated proteins accumulated in both *amsh3* and AMSH3(AXA)-overexpressing plants are indeed membrane associated and might represent membrane cargos.

Enzymatic inactive AMSH inhibits CERK1 degradation

To examine whether AMSH DUB activity can affect the stability of known endocytic cargo proteins, we next analyzed the AvrPtoB-dependent endocytic degradation of CERK1 in a

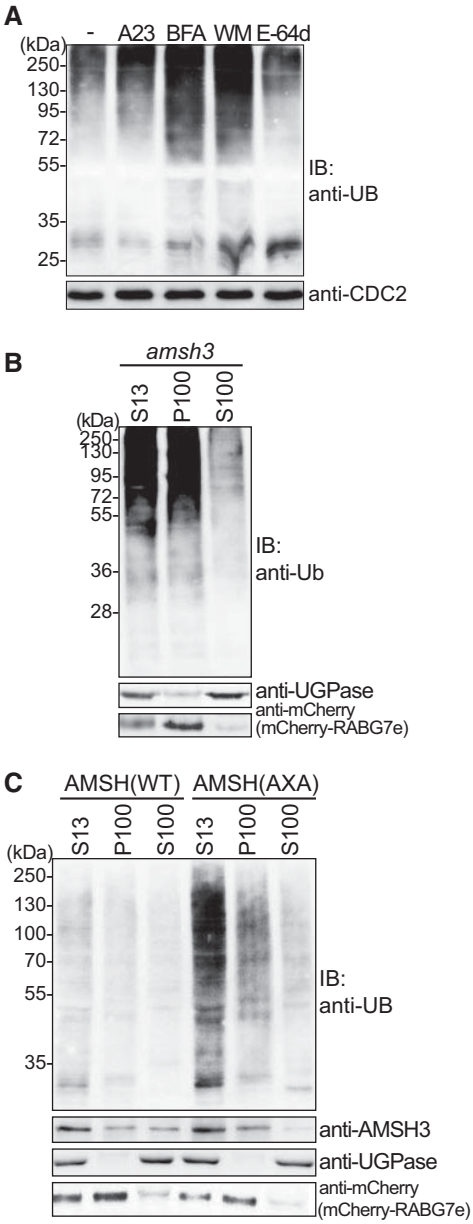

Fig. 3 Ubiquitinated proteins accumulate in the membrane fraction in *amsh3* mutants. (A) Seven-day-old wild-type seedlings were treated with A23, BFA and WM for 12 h. Total extracts were subjected to immunoblotting with an anti-ubiquitin antibody. CDC2 was used as a loading control. (B) Total extracts (S13) of 7-day-old *amsh3* mutants were fractionated by ultracentrifugation to separate the microsomal fraction (P100) and soluble fraction (S100) and subjected to immunoblotting using an anti-ubiquitin antibody. Note that the majority of ubiquitinated proteins accumulate in the membrane (P100) fraction. (C) Seven-day-old DEX-inducible AMSH3(WT) and AMSH3(AXA) lines were incubated in liquid medium supplemented with DEX for 20 h. Total extracts of DEX-induced seedlings (S13) were fractionated by ultracentrifugation to separate the microsomal fraction (P100) and soluble fraction (S100), and subsequently subjected to immunoblotting with anti-ubiquitin and anti-AMSH3 ntibodies.

transient system. AvrPtoB is a type III effector protein possessing E3 ubiquitin ligase activity that is secreted by the bacterial pathogen *Pseudomonas syringae* to suppress plant immunity (Abramovitch et al. 2006, Gimenez-Ibanez et al. 2009). AvrptoB-dependent ubiquitination and degradation of the Arabidopsis plasma membrane receptor CERK1 can be reconstituted by transient expression in *Nicotiana benthamiana* leaves (Gimenez-Ibañez et al. 2009). We used this system to test whether AMSH enzymes play a role in CERK1 turnover. We expressed the enzymatically inactive, dominant-negative, AMSH1(AXA) and AMSH3(AXA) constructs under an ethanol-inducible promoter, together with AvrPtoB and CERK1. Without ethanol, CERK1-HA was rapidly degraded in the presence of AvrPtoB, as previously reported (Gimenez-Ibañez et al. 2009). Importantly, ethanol-induced expression of the AXA constructs completely inhibited AvrPtoB-directed CERK1-HA degradation (**Fig. 5**), indicating that AMSH enzymes are required for endocytic degradation of this receptor. Furthermore, expression of the AXA constructs also increased the levels of CERK1 accumulation in the absence of AvrptoB, suggesting that there is a basal rate of AMSH-dependent CERK1 degradation even when the bacterial effector is not present.

AMSH3 co-fractionates with ubiquitinated proteins

Next we wanted to examine the cellular compartment where the ubiquitinated proteins and AMSH3 localize. For this purpose, we performed size exclusion chromatography from total extracts of seedlings overexpressing AMSH3(AXA). AMSH3 mostly appears as a monomeric protein in lower molecular weight fractions, not associated with high molecular weight complexes. However, a small portion of AMSH3(AXA) and ubiquitinated proteins co-elute at a higher molecular weight (**Fig. 4A**), suggesting that they might be associated with cellular organelles. To investigate whether AMSH3 co-fractionates with known organelle markers, we therefore further performed a sucrose gradient fractionation from the membrane fraction (P100) obtained from Arabidopsis cell culture. AMSH3 does not show a clear co-fractionation with any of the tested markers (V-ATPase, BiP, SEC21 and CHC) (**Fig. 4B**) under this condition, suggesting that AMSH3 is not a stable component of the vacuole, endoplasmic reticulum, Golgi or clathrin-positive endosomal membranes.

The MIT domain of AMSH3 is essential for direct interaction with the ESCRT-III subunit VPS2.1

Although we could not find evidence for stable interaction of AMSH3 with specific cellular structures, AMSH3 were previously shown to interact directly with ESCRT-III subunits VPS2.1 and VPS24.1 (Katsiarimpa et al. 2011). To examine the importance of this interaction in planta, we carried out mutational analysis of the ESCRT-III–AMSH3 binding domain. It was previously shown that a mutation in the VPS2.1 C-terminal MIM disrupts the interaction between VPS2.1 and

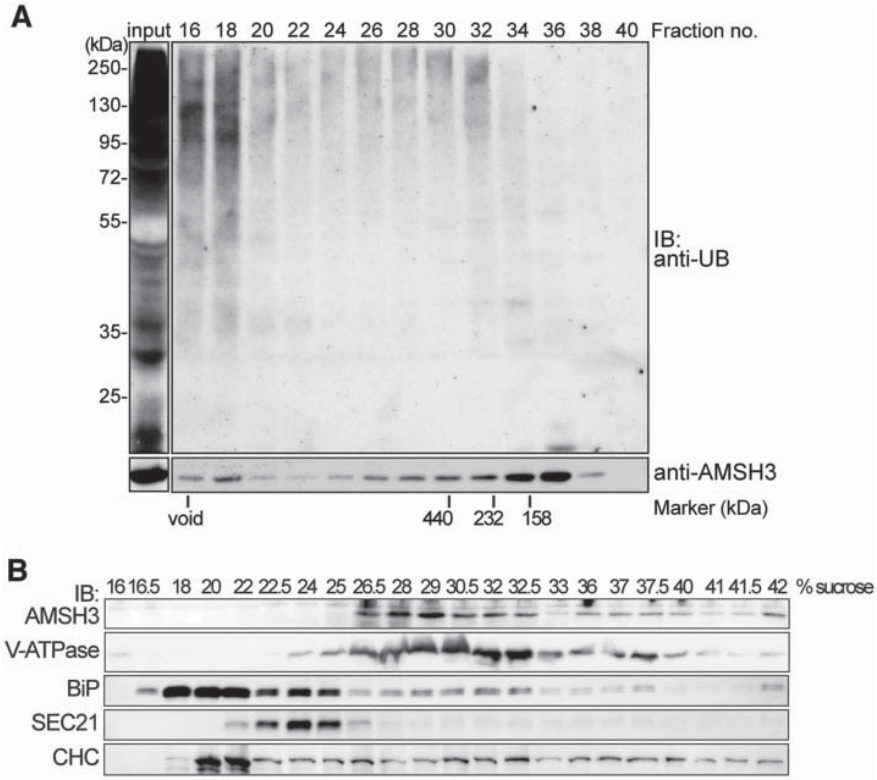

Fig. 4 AMSH3 does not co-fractionate with vacuole, endoplasmic reticulum or Golgi markers. (A) Total protein extracts of AMSH3(AXA)-expressing seedlings were subjected to gel filtration chromatography. Fractions of 500 µl were collected and subjected to immunoblotting using anti-ubiquitin and anti-AMSH3 antibodies. The positions of marker proteins are indicated on the bottom. (B) The microsomal fraction (P100) prepared from Arabidopsis cell culture was fractionated over a 15–45% sucrose gradient. Samples of each fraction were analyzed by immunoblot using anti-AMSH3, anti-V-ATPase (vacuole), anti-BiP (endoplasmic reticulum), anti-SEC21 (Golgi) and anti-CHC antibodies. Sucrose concentrations in each fraction are indicated on top of the panels.

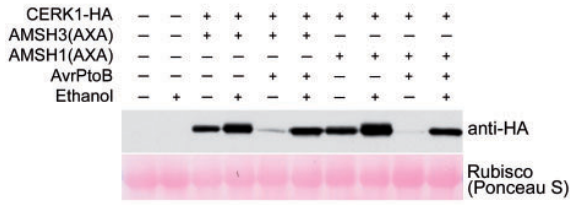

Fig. 5 Expression of DUB-inactive AMSH stabilizes CERK1. CERK1-HA-, AMSH3(AXA)-, AMSH1(AXA)- and AvrPtoB-expressing constructs were transformed in *Nicotiana* leaves and expression of AMSH3(AXA) and AMSH1(AXA) was induced by ethanol. Total extracts from leaf discs were analyzed by immunoblotting with an anti-HA antibody. A protein band corresponding to Rubisco stained with Ponceau S is shown as a loading control.

AMSH3, indicating the importance of this domain for the interaction with AMSH3. To establish whether the MIM of VPS2.1 is sufficient for the interaction, we purified glutathione S-transferase (GST)-fused MIM of VPS2.1 [GST–VPS2.1(MIM)] [(**Supplementary Fig. S2**) and performed an in vitro binding assay with full-length AMSH3 or GST. GST–VPS2.1(MIM), but not the GST moiety alone, could pull-down AMSH3, indicating that the MIM region of VPS2.1 is indeed sufficient for the interaction (**Fig. 6A, B**).

To verify that the MIT domain is required for the direct interaction between AMSH3 and VPS2.1, we again performed an in vitro binding assay with recombinant GST–VPS2.1 or GST and AMSH3 without the MIT domain [AMSH3(ΔMIT)]. When GST–VPS2.1 and GST were incubated with either full-length AMSH3 or AMSH3(ΔMIT), only full-length AMSH3, but not AMSH3(ΔMIT) was pulled-down by GST–VPS2.1 (**Fig. 6B, C**; **Supplementary Fig. S3**), indicating that the MIT domain is necessary for the direct interaction between the ESCRT-III subunit VPS2.1 and AMSH3. The MIT domain is not essential for the DUB activity of AMSH3, since AMSH3(ΔMIT) was still able to cleave K48- and K63-linked ubiquitin chains in a DUB assay (**Fig. 6D**).

The MIT domain is necessary for AMSH3 function in vivo

We next wanted to investigate whether the interaction with ESCRT-III is important for AMSH3 function and to test whether the MIT domain is essential for AMSH3 function in vivo. Since

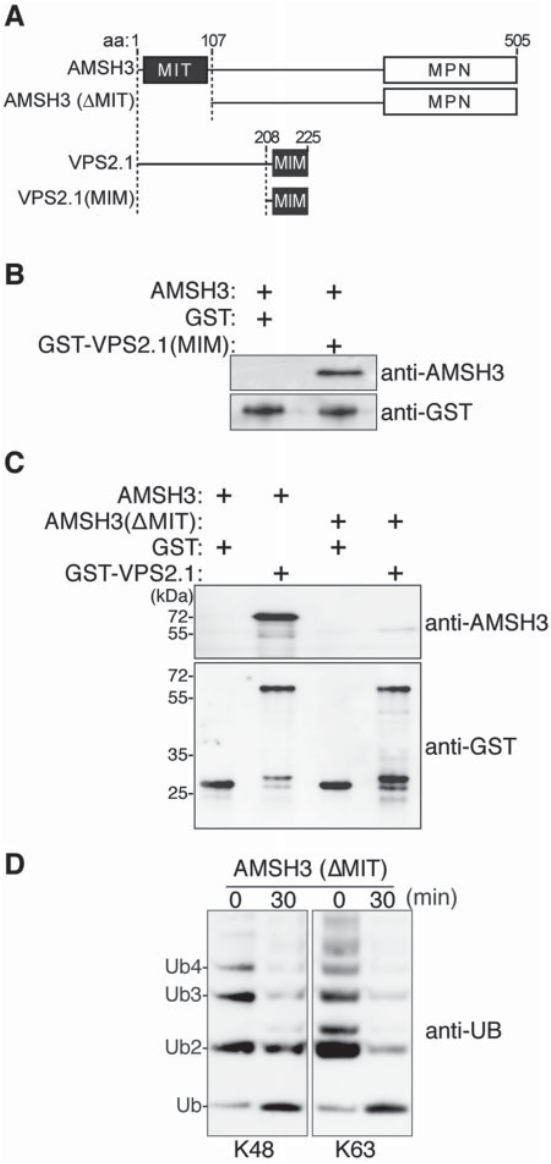

Fig. 6 The MIT domain of AMSH3 is required for AMSH3 function in vivo. (A) Construct used for in vitro binding assays. (B) In vitro binding assay with GST, GST–VPS2.1(MIM) and AMSH3. After GST pull-down, bead-bound proteins were analyzed by immunoblotting using anti-AMSH3 and anti-GST antibodies. (C) In vitro binding assay with GST, GST–VPS2.1, AMSH3 and AMSH3(ΔMIT). As in (B), bead-bound proteins were analyzed using anti-AMSH3 and anti-GST antibodies. (D) In vitro DUB assay. Purified AMSH3(ΔMIT) (2 pmol) was incubated with 250 ng of either K48- or K63-linked ubiquitin chains (Ub_{2-7}) for 30 min. Hydrolysis of the ubiquitin chains was analyzed on an immunoblot using an anti-ubiquitin antibody. The positions of mono-, di-, tri- and tetraubiquitin are indicated on the left.

we could not recover transgenic plants overexpressing HA-AMSH3(ΔMIT), we generated a dexamethasone (DEX)-inducible AMSH3(ΔMIT) construct and transformed this into *amsh3* mutants. The expression of AMSH3(WT) in *amsh3* upon

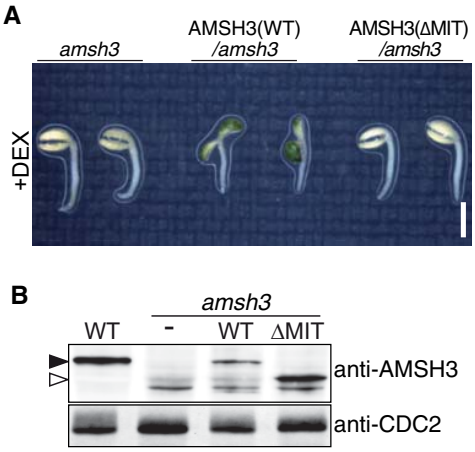

Fig. 7 AMSH3(ΔMIT) does not complement the *amsh3* mutant phenotype. (A) *amsh3* mutants with either DEX-inducible AMSH3(WT) or AMSH3(ΔMIT) constructs were grown on 30 μM dexamethasone-containing plates for 7 d. Scale bar = 2 mm. Note that in contrast to AMSH3(WT), *amsh3* mutants expressing AMSH3(ΔMIT) do not show a partial complementation. (B) Total proteins were extracted from seedlings in (A) and subjected to immunoblot analysis with an anti-AMSH3 antibody. CDC2 was used as a loading control. Solid arrowhead, position of the full-length AMSH3; open arrowhead, position of AMSH3(ΔMIT).

germination, in contrast to 35S:HA-AMSH3 (Isono et al. 2010), does not completely complement the developmental phenotype of *amsh3* (**Fig. 7A, B**), indicating that AMSH3 function is essential already before germination, probably during embryogenesis. Nonetheless, when AMSH3(WT) is expressed in an *amsh3* background, cotyledons opened and became green, which normally does not happen in *amsh3* mutants. In contrast, *amsh3* mutants expressing AMSH3(ΔMIT) remained white and its cotyledons did not open even though the AMSH3(ΔMIT) protein could be detected by immunoblotting (**Fig. 7A, B**). This result shows that the MIT domain, and hence the interaction of AMSH3 with ESCRT-III subunits, is essential for AMSH3 function in vivo.

Discussion

In this study, we demonstrated that the *amsh3* function is important for efficient endocytic degradation. Considering the interaction of AMSH3 with ESCRT-III (Katsiarimpa et al. 2011) and the necessity for the ESCRT-III-interacting MIT domain of AMSH3 for its in planta protein function, we could suggest that AMSH3 function in intracellular trafficking is dependent on its interaction with the ESCRT-III machinery. In order to come into physical proximity and deubiquitinate its membrane-localized substrate proteins, AMSH3 probably must be recruited to the late endosomes/MVBs through the interaction with ESCRT-III subunits.

MIT domains can be found in proteins that in most of the cases interact with ESCRT-III subunits. Although MIT domains

from different proteins have a broad variety of primary sequences, they serve as binding surfaces for the MIM found in multiple ESCRT-III subunits (Obita et al. 2007, Stuchell-Brereton et al. 2007, Azmi et al. 2008, Xiao et al. 2008). Structural analysis of co-crystallized human AMSH(MIT) and CHMP3/VPS24(MIM) has revealed a strong affinity between AMSH and CHMP3 (Solomons et al. 2011). Furthermore, mutations in the binding surface affecting the AMSH3–CHMP3 interaction lead to loss of AMSH function in vivo. Sequence analysis indicates that the AMSH3–ESCRTIII interaction is conserved in higher eukaryotes, since the MIT domain of AMSH3 and the MIM of ESCRT-III subunits are conserved across the kingdom (Katsiarimpa et al. 2011). In contrast to yeast, in which ESCRT-III subunits were first identified and characterized and in which only one gene is coding for each subunit, multiple homologs exist for each ESCRT-III subunit in higher eukaryotes, especially in plants, implying functional diversification (Winter and Hauser 2006). It is intriguing to postulate that different ESCRT-III complexes with different homolog composition carry out their specific roles in higher plants, especially since interaction studies have shown that different homologs can have different interaction partners within the plant ESCRT-III complex (Ibl et al. 2011, Richardson et al. 2011, Shahriari et al. 2011). Future studies will have to reveal the functional and spatio-temporal differentiation of ESCRT-III homologs, how their complex formation is coordinated at the molecular level and how the recruitment of DUBs to endosomal membranes is regulated.

Although cargo ubiquitination is a trigger for endocytosis and is important for cargo trafficking to the vacuole, cargo deubiquitination does not seem to be crucial for cargo degradation per se, at least in protoplasts. Two recent publications have shown that the translational, and hence not hydrolyzable, fusion of a single ubiquitin molecule is enough for cargo transport to the vacuole (Herberth et al. 2012, Scheuring et al. 2012). Nonetheless, AMSH3 interaction with ESCRT-III as well as AMSH3 DUB activity seem to be essential for proper plant development. In yeast, a DUB mutant *doa4Δ* shows decreased viability in the stationary phase and depletion of free ubiquitin. This phenotype of *doa4Δ* could be partially rescued by overexpression of ubiquitin. Therefore, it was suggested some time ago that Doa4p function, and generally DUB function, in endocytosis is mainly to maintain the free ubiquitin pool for conjugation (Swaminathan et al. 1999). However, more detailed analysis has revealed that the *doa4* mutant phenotype cannot be solely explained by the low abundance of free ubiquitin (Nikko and Andre 2007). Interestingly, in contrast to yeast *doa4Δ* mutants, *AMSH* mutants do not show a significant reduction in the amount of free ubiquitin in the first place (Isono et al. 2010, Katsiarimpa et al. 2013). AMSH DUB function may therefore be required for more specific processes in regulating substrate stability during endocytosis in plant.

Pharmaceutical inhibition of endocytosis also leads to accumulation of ubiquitinated proteins, as well as in *amsh1* and *amsh3* mutants or *VPS2.1* dominant-negative mutants (Isono et al. 2010, Katsiarimpa et al. 2013). Ubiquitinated proteins that accumulate in *amsh3* are found in the microsomal fraction and thus can be plasma membrane proteins and/or membrane-bound endocytosis machinery. Though identification of DUB substrates is generally not trivial due to its broad target spectra, it would be a future challenge to identify the nature of these ubiquitinated proteins.

Materials and Methods

Biological material

All experiments were performed in the *A. thaliana* Columbia-0 background. Plant transformations were carried out using the floral dip method (Clough and Bent 1998). Seedlings were grown in continuous light, at 110–120 $\mu mol\ m^{-2}\ s^{-1}$ light intensity. Standard Murashige and Skoog (MS) growth medium (Duchefa Biochemie) (2.15 $g\ l^{-1}$ MS, 2.3 mM MES, pH 5.7) supplemented with 1% sucrose was used to grow seedlings. Adult plants were grown on soil. For DEX induction, a final concentration of 30 μM DEX (Duchefa) was added to the medium. PIN2:PIN2–GFP (Abas et al. 2006) was previously published. For drug treatment, 11-day-old seedlings were treated with 20 μM tyrphostin A23 (Sigma Aldrich), 25 μM BFA (Fisher Scientific), 20 μM WM (Applichem) or 100 μM E-64d (Santa Cruz) for 12 h.

Cloning procedures

All primers used for cloning and subcloning are listed in **Supplementary Table S1**. To yield GST–AMSH3(ΔMIT) and DEX:AMSH3(ΔMIT), a fragment of AMSH3 was amplified using primers 5′-AAGGGGATCCGAGGATGAATCCCGTCA-3′ and 5′-AAGGGCGGCCGGTTAGCGGAGATCGAGGA-3′ or 5′-AAGGCTCGAGATGGATGAATCCCGTCAGGAT-3′ and 5′-AAGGACTAGTTTAGCGGAGATCGAGGAC-3′, respectively, and cloned between the *Bam*HI and *Not*I sites of pGEX6P1 (Healthcare Life Sciences) or between the *Xho*I and *Spe*I sites of pTA7002 (Aoyama and Chua 1997), respectively. AMSH1(AXA) and AMSH3(AXA) were cloned into vector pBINSRNA for ethanol-inducible expression.

CERK1 degradation assay

For the transformation of *N. benthamiana*, Agrobacterium cells in late exponential phase (<20 h growth in liquid medium) were harvested by centrifugation and resuspended in infiltration buffer containing 10 mM MES-KOH (pH 5.6), 10 mM $MgCl_2$ and 150 μM acetosyringone), diluted to an optical density at 600 nm of 0.3 and mixed according to the different experiments. Bacteria were injected into leaves of 5-week-old *N. benthamiana* plants. Two days after infiltration, plants were covered with a plastic bag, with or without an open 1.5 ml tube containing ethanol to produce ethanol vapors for the induction of the expression of AMSH3(AXA) or AMSH1(AXA). The leaf discs of the infiltrated leaves were harvested after overnight

induction and frozen in liquid nitrogen. Proteins were extracted with SDS–PAGE loading buffer.

Protein extraction and western blotting

Total protein extracts were prepared in extraction buffer (50 mM Tris–HCl, pH 7.5, 150 mM NaCl, 0.5% Triton X-100) supplemented with protease inhibitor cocktail (Roche). SDS–PAGE and immunoblotting were performed according to standard methods. Antibodies used are: anti-AMSH3 (Isono et al. 2010), anti-CDC2 (Santa Cruz), anti-HA (Roche), anti-mCherry (MBL), anti-UB (Santa Cruz), anti-UGPase (Agrisera), anti-CHC (Agrisera), anti-V-ATPase (Agrisera), anti-SEC21 (Agrisera) and anti-BiP (Enzo Life Sciences). Protein purification and in vitro binding assay were performed as described previously (Katsiarimpa et al. 2011). *The i*n vitro DUB assay was performed as described previously (Isono et al. 2010).

Ultracentrifugation, gel filtration and sucrose gradient fractionation

To separate the microsomal (P100) from the soluble (S100) fraction, ultracentrifugation was performed as described previously (Isono et al. 2010). Gel filtration with a Superose 6 (GE Healthcare Life Sciences) column was performed with 2 mg of plant total extracts as described before (Isono et al. 2004). Sucrose density gradient centrifugation of the membrane fraction (P100) was performed on a linear sucrose gradient. Arabidopsis cultured cells were collected from 100 ml of culture and washed twice with WD buffer (0.4 M mannitol, 8 mM $CaCl_2$). Cells were protoplasted by incubation in WD buffer containing 1% cellulase and 0.25% macerozyme for 3 h as described before (Katsiarimpa et al. 2011). Protoplasts were washed twice with WD buffer and homogenized using a glass tube and a pestle, centrifuged at 2,000 $\times$ *g* for 20 min at 4°C and the supernatant was used for ultracentrifugation at 100,000 $\times$ *g* to yield the P100 pellet. The P100 pellet was dissolved in 600 µl of sucrose buffer (400 mM sucrose, 50 mM HEPES-KOH pH 7.5, 10 mM KCl, 1 mM EDTA pH 7.5), loaded on top of a linear 15–45% sucrose gradient and centrifuged at 150,000 $\times$ *g* for 16 h. Fractions of 200 µl were collected from top to bottom and proteins in each fraction were subsequently precipitated by trichloroacetic acid. The sucrose concentration in each fraction was determined by a refractometer.

Microscopy

GFP-fused proteins were analyzed with an FV-1000/IX81 confocal laser scanning microscope (Olympus) with a UPlanSApo X60/1.20 (Olympus) objective using the 488 nm laser line. For FM4-64 staining, seedlings were incubated with 2 µM FM4-64 for 10 min before observation. BFA (Fisher Scientific) and WM (Applichem) were added at a final concentration of 50 µM and 33 µM, respectively, in liquid media. Images were processed and quantified using Fluoview (Olympus) and Photoshop CS6 (Adobe).

Supplementary data

Supplementary data are available at PCP online.

Funding

This work was supported by the Deutsche Forschungsgemeinschaft [IS221/2-2 to E.I.] and by the Spanish Ministry of Research, Development and Innovation [BIO2012-39968 to E.R.].

Acknowledgments

We would like to thank John Rathjen (The Australian National University, Australia) for the CERK1-HA and AvrPtoB vectors, and Daniela Dyckhof, Sebastian Wenz and Franziska Anzenberger (Technische Universität München) for technical support.

Disclosures

The authors have no conflicts of interest to declare.

References

Abas, L., Benjamins, R., Malenica, N., Paciorek, T., Wisniewska, J., Moulinier-Anzola, J.C. et al. (2006) Intracellular trafficking and proteolysis of the Arabidopsis auxin-efflux facilitator PIN2 are involved in root gravitropism. *Nat. Cell Biol.* 8: 249–256.

Abramovitch, R.B., Janjusevic, R., Stebbins, C.E. and Martin, G.B. (2006) Type III effector AvrPtoB requires intrinsic E3 ubiquitin ligase activity to suppress plant cell death and immunity. *Proc. Natl Acad. Sci. USA* 103: 2851–2856.

Ambroggio, X.I., Rees, D.C. and Deshaies, R.J. (2004) JAMM: a metallo-protease-like zinc site in the proteasome and signalosome. *PLoS Biol.* 2: E2.

Aoyama, T. and Chua, N.H. (1997) A glucocorticoid-mediated transcriptional induction system in transgenic plants. *Plant J.* 11: 605–612.

Azmi, I.F., Davies, B.A., Xiao, J., Babst, M., Xu, Z. and Katzmann, D.J. (2008) ESCRT-III family members stimulate Vps4 ATPase activity directly or via Vta1. *Dev. Cell* 14: 50–61.

Barberon, M., Zelazny, E., Robert, S., Conejero, G., Curie, C., Friml, J. et al. (2011) Monoubiquitin-dependent endocytosis of the iron-regulated transporter 1 (IRT1) transporter controls iron uptake in plants. *Proc. Natl Acad. Sci. USA* 108: E450–E458.

Clague, M.J. and Urbe, S. (2006) Endocytosis: the DUB version. *Trends Cell Biol.* 16: 551–559.

Clough, S.J. and Bent, A.F. (1998) Floral dip: a simplified method for Agrobacterium-mediated transformation of *Arabidopsis thaliana*. *Plant J.* 16: 735–743.

Dhonukshe, P., Aniento, F., Hwang, I., Robinson, D.G., Mravec, J., Stierhof, Y.D. et al. (2007) Clathrin-mediated constitutive endocytosis of PIN auxin efflux carriers in Arabidopsis. *Curr. Biol.* 17: 520–527.

Doelling, J.H., Phillips, A.R., Soyler-Ogretim, G., Wise, J., Chandler, J., Callis, J. et al. (2007) The ubiquitin-specific protease subfamily

UBP3/UBP4 is essential for pollen development and transmission in Arabidopsis. *Plant Physiol.* 145: 801–813.
Doelling, J.H., Yan, N., Kurepa, J., Walker, J. and Vierstra, R.D. (2001) The ubiquitin-specific protease UBP14 is essential for early embryo development in Arabidopsis thaliana. *Plant J.* 27: 393–405.
Geldner, N., Denervaud-Tendon, V., Hyman, D.L., Mayer, U., Stierhof, Y.-D. and Chory, J. (2009) Rapid, combinatorial analysis of membrane compartments in intact plants with a multicolor marker set. *Plant J.* 59: 169–178.
Geldner, N., Friml, J., Stierhof, Y.D., Jurgens, G. and Palme, K. (2001) Auxin transport inhibitors block PIN1 cycling and vesicle trafficking. *Nature* 413: 425–428.
Gimenez-Ibanez, S., Hann, D.R., Ntoukakis, V., Petutschnig, E., Lipka, V. and Rathjen, J.P. (2009) AvrPtoB targets the LysM receptor kinase CERK1 to promote bacterial virulence on plants. *Curr. Biol.* 19: 423–429.
Gohre, V., Spallek, T., Haweker, H., Mersmann, S., Mentzel, T., Boller, T. et al. (2008) Plant pattern-recognition receptor FLS2 is directed for degradation by the bacterial ubiquitin ligase AvrPtoB. *Curr. Biol.* 18: 1824–1832.
Hasdemir, B., Murphy, J.E., Cottrell, G.S. and Bunnett, N.W. (2009) Endosomal deubiquitinating enzymes control ubiquitination and down-regulation of protease-activated receptor 2. *J. Biol. Chem.* 284: 28453–28466.
Herberth, S., Shahriari, M., Bruderek, M., Hessner, F., Muller, B., Hulskamp, M. et al. (2012) Artificial ubiquitylation is sufficient for sorting of a plasma membrane ATPase to the vacuolar lumen of Arabidopsis cells. *Planta* 236: 63–77.
Huang, F., Zeng, X., Kim, W., Balasubramani, M., Fortian, A., Gygi, S.P. et al. (2013) Lysine 63-linked polyubiquitination is required for EGF receptor degradation. *Proc. Natl Acad. Sci. USA* 110: 15722–15727.
Ibl, V., Csaszar, E., Schlager, N., Neubert, S., Spitzer, C. and Hauser, M.T. (2011) Interactome of the plant-specific ESCRT-III component AtVPS2.2 in Arabidopsis thaliana. *J. Proteome Res.* 11: 397–411.
Ishii, N., Owada, Y., Yamada, M., Miura, S., Murata, K., Asao, H. et al. (2001) Loss of neurons in the hippocampus and cerebral cortex of AMSH-deficient mice. *Mol. Cell Biol.* 21: 8626–8637.
Isono, E., Katsiarimpa, A., Muller, I.K., Anzenberger, F., Stierhof, Y.D., Geldner, N. et al. (2010) The deubiquitinating enzyme AMSH3 is required for intracellular trafficking and vacuole biogenesis in Arabidopsis thaliana. *Plant Cell* 22: 1826–1837.
Isono, E., Saeki, Y., Yokosawa, H. and Toh-e, A. (2004) Rpn7 is required for the structural integrity of the 26S proteasome of *Saccharomyces cerevisiae*. *J. Biol. Chem.* 279: 27168–27176.
Jaillais, Y., Fobis-Loisy, I., Miege, C., Rollin, C. and Gaude, T. (2006) AtSNX1 defines an endosome for auxin-carrier trafficking in Arabidopsis. *Nature* 443: 106–109.
Kasai, K., Takano, J., Miwa, K., Toyoda, A. and Fujiwara, T. (2011) High boron-induced ubiquitination regulates vacuolar sorting of the BOR1 borate transporter in Arabidopsis thaliana. *J. Biol. Chem.* 286: 6175–6183.
Katsiarimpa, A., Anzenberger, F., Schlager, N., Neubert, S., Hauser, M.T., Schwechheimer, C. et al. (2011) The Arabidopsis deubiquitinating enzyme AMSH3 interacts with ESCRT-III subunits and regulates their localization. *Plant Cell* 23: 3026–3040.
Katsiarimpa, A., Kalinowska, K., Anzenberger, F., Weis, C., Ostertag, M., Tsutsumi, C. et al. (2013) The deubiquitinating enzyme AMSH1 and the ESCRT-III subunit VPS2.1 are required for autophagic degradation in Arabidopsis. *Plant Cell* 25: 2236–2252.
Komander, D., Clague, M.J. and Urbe, S. (2009) Breaking the chains: structure and function of the deubiquitinases. *Nat. Rev. Mol. Cell Biol.* 10: 550–563.
Lee, H.K., Cho, S.K., Son, O., Xu, Z., Hwang, I. and Kim, W.T. (2009) Drought stress-induced Rma1H1, a RING membrane-anchor E3 ubiquitin ligase homolog, regulates aquaporin levels via ubiquitination in transgenic Arabidopsis plants. *Plant Cell* 21: 622–641.
Liu, Y., Wang, F., Zhang, H., He, H., Ma, L. and Deng, X.W. (2008) Functional characterization of the Arabidopsis ubiquitin-specific protease gene family reveals specific role and redundancy of individual members in development. *Plant J.* 55: 844–856.
Luo, M., Luo, M.Z., Buzas, D., Finnegan, J., Helliwell, C., Dennis, E.S. et al. (2008) UBIQUITIN-SPECIFIC PROTEASE 26 is required for seed development and the repression of PHERES1 in Arabidopsis. *Genetics* 180: 229–236.
Ma, Y.M., Boucrot, E., Villen, J., Affar el, B., Gygi, S.P., Gottlinger, H.G. et al. (2007) Targeting of AMSH to endosomes is required for epidermal growth factor receptor degradation. *J. Biol. Chem.* 282: 9805–9812.
Maytal-Kivity, V., Reis, N., Hofmann, K. and Glickman, M.H. (2002) MPN+, a putative catalytic motif found in a subset of MPN domain proteins from eukaryotes and prokaryotes, is critical for Rpn11 function. *BMC Biochem.* 3: 28.
McCullough, J., Clague, M.J. and Urbe, S. (2004) AMSH is an endosome-associated ubiquitin isopeptidase. *J. Cell Biol.* 166: 487–492.
McCullough, J., Row, P.E., Lorenzo, O., Doherty, M., Beynon, R., Clague, M.J. et al. (2006) Activation of the endosome-associated ubiquitin isopeptidase AMSH by STAM, a component of the multivesicular body-sorting machinery. *Curr. Biol.* 16: 160–165.
Nikko, E. and Andre, B. (2007) Evidence for a direct role of the Doa4 deubiquitinating enzyme in protein sorting into the MVB pathway. *Traffic* 8: 566–581.
Obita, T., Saksena, S., Ghazi-Tabatabai, S., Gill, D.J., Perisic, O., Emr, S.D. et al. (2007) Structural basis for selective recognition of ESCRT-III by the AAA ATPase Vps4. *Nature* 449: 735–739.
Richardson, L.G., Howard, A.S., Khuu, N., Gidda, S.K., McCartney, A., Morphy, B.J. et al. (2011) Protein–protein interaction network and subcellular localization of the Arabidopsis thaliana ESCRT machinery. *Front. Plant Sci.* 2: 20.
Sato, Y., Yoshikawa, A., Yamagata, A., Mimura, H., Yamashita, M., Ookata, K. et al. (2008) Structural basis for specific cleavage of Lys 63-linked polyubiquitin chains. *Nature* 455: 358–362.
Schellmann, S. and Pimpl, P. (2009) Coats of endosomal protein sorting: retromer and ESCRT. *Curr. Opin. Plant Biol.* 12: 670–676.
Scheuring, D., Kunzl, F., Viotti, C., Yan, M.S., Jiang, L., Schellmann, S. et al. (2012) Ubiquitin initiates sorting of Golgi and plasma membrane proteins into the vacuolar degradation pathway. *BMC Plant Biol.* 12: 164.
Schmitz, R.J., Tamada, Y., Doyle, M.R., Zhang, X. and Amasino, R.M. (2009) Histone H2B deubiquitination is required for transcriptional activation of FLOWERING LOCUS C and for proper control of flowering in Arabidopsis. *Plant Physiol.* 149: 1196–1204.
Shahriari, M., Richter, K., Keshavaiah, C., Sabovljevic, A., Huelskamp, M. and Schellmann, S. (2011) The Arabidopsis ESCRT protein–protein interaction network. *Plant Mol. Biol.* 76: 854–96.
Sierra, M.I., Wright, M.H. and Nash, P.D. (2010) AMSH interacts with ESCRT-0 to regulate the stability and trafficking of CXCR4. *J. Biol. Chem.* 285: 13990–14004.

Solomons, J., Sabin, C., Poudevigne, E., Usami, Y., Hulsik, D.L., Macheboeuf, P. et al. (2011) Structural basis for ESCRT-III CHMP3 recruitment of AMSH. *Structure* 19: 1149–1159.

Spitzer, C., Reyes, F.C., Buono, R., Sliwinski, M.K., Haas, T.J. and Otegui, M.S. (2009) The ESCRT-related CHMP1A and B proteins mediate multivesicular body sorting of auxin carriers in Arabidopsis and are required for plant development. *Plant Cell* 21: 749–766.

Spitzer, C., Schellmann, S., Sabovljevic, A., Shahriari, M., Keshavaiah, C., Bechtold, N. et al. (2006) The Arabidopsis *elch* mutant reveals functions of an ESCRT component in cytokinesis. *Development* 133: 4679–4689.

Sridhar, V.V., Kapoor, A., Zhang, K., Zhu, J., Zhou, T., Hasegawa, P.M. et al. (2007) Control of DNA methylation and heterochromatic silencing by histone H2B deubiquitination. *Nature* 447: 735–738.

Stuchell-Brereton, M.D., Skalicky, J.J., Kieffer, C., Karren, M.A., Ghaffarian, S. and Sundquist, W.I. (2007) ESCRT-III recognition by VPS4 ATPases. *Nature* 449: 740–744.

Swaminathan, S., Amerik, A.Y. and Hochstrasser, M. (1999) The Doa4 deubiquitinating enzyme is required for ubiquitin homeostasis in yeast. *Mol. Biol. Cell* 10: 2583–2594.

Tanaka, N., Kaneko, K., Asao, H., Kasai, H., Endo, Y., Fujita, T. et al. (1999) Possible involvement of a novel STAM-associated molecule 'AMSH' in intracellular signal transduction mediated by cytokines. *J. Biol. Chem.* 274: 19129–19135.

Teis, D., Saksena, S. and Emr, S.D. (2008) Ordered assembly of the ESCRT-III complex on endosomes is required to sequester cargo during MVB formation. *Dev. Cell* 15: 578–589.

Williams, R.L. and Urbe, S. (2007) The emerging shape of the ESCRT machinery. *Nat. Rev. Mol. Cell Biol.* 8: 355–368.

Winter, V. and Hauser, M.T. (2006) Exploring the ESCRTing machinery in eukaryotes. *Trends Plant Sci.* 11: 115–123.

Xiao, J., Xia, H., Zhou, J., Azmi, I.F., Davies, B.A., Katzmann, D.J. et al. (2008) Structural basis of Vta1 function in the multivesicular body sorting pathway. *Dev. Cell* 14: 37–49.

Yan, N., Doelling, J.H., Falbel, T.G., Durski, A.M. and Vierstra, R.D. (2000) The ubiquitin-specific protease family from Arabidopsis. AtUBP1 and 2 are required for the resistance to the amino acid analog canavanine. *Plant Physiol.* 124: 1828–1843.